Open Journal of Energy Efficiency, 2022, 11, 122-141
https://www.scirp.org/journal/ojee
ISSN Online: 2169-2645
ISSN Print: 2169-2637

Experimental and Simulation Validation of Piezoelectric Road Energy Harvesting

Andrew Sherren, Kyle Fink, Joshua Eshelman, Luay Yassin Taha, Sohail Anwar, Craig Brennecke, Hussein M. Abdeltawab, Shihui Shen, Faeze Ghofrani, Cheng Zhang

College of Engineering, The Pennsylvania State University, Altoona, USA
Email: lqt5312@@psu.edu

How to cite this paper: Sherren, A., Fink, K., Eshelman, J., Taha, L.Y., Anwar, S., Brennecke, C., Abdeltawab, H.M., Shen, S.H., Ghofrani, F. and Zhang, C. (2022) Experimental and Simulation Validation of Piezoelectric Road Energy Harvesting. *Open Journal of Energy Efficiency*, **11**, 122-141.
https://doi.org/10.4236/ojee.2022.113009

Received: July 22, 2022
Accepted: September 23, 2022
Published: September 26, 2022

Abstract

This project strived to develop a prototype road piezoelectric energy harvester RPEH system using five Lead Zirconate Titanate (PZT) PZT 5H modules (stacks) that are embedded in the road by means of a housing unit to harvest energy from vehicles stressing the modules. The work is an extension of our previous published work in the same journal. The design considered many factors to optimize the harvested energy. The proposed system first captures mechanical energy using a designed module that transfers the energy to the piezoelectric stacks. Then the captured energy will be converted into electrical energy by the piezoelectric phenomenon. The harvested energy is stored in a storage device, then analyzed by an oscilloscope through the acquisition of the harvested voltage, current, power, and energy. When testing the RPEH with the wheel tracking machine, varying resistor loads where connected to the output of the RPEH to address the optimum power delivered to the load. The optimum load was found to be 950 kΩ, and the optimal harvested energy was recorded as 45 uJ.

Keywords

Energy Harvesting, Piezoelectric Harvesters, Road Pavement, Device Modelling

1. Introduction

Recently, there is an increasing demand for designing and developing of smart highways and roads that harvest energy from piezoelectric harvester to control and minimize the energy consumption, save energy, and reduce cost, CO_2 emission, and risks [1].

This paper is an extension of our previous published work in the same journal

[1], and aimed to develop a RPEH system, based on using five Lead Zirconate Titanate (PZT)PZT 5H modules (stacks) that are embedded in the road to harvest energy from the vehicles stressing the modules. The design considered many factors to optimize the harvested energy. The proposed system first captures the mechanical energy using the piezoelectric stacks. Then the captured energy will be converted into electrical energy by piezoelectric phenomenon. The harvested energy is stored in a storage device, then analyzed by a computer through the acquisition of the harvested voltage, current, power, and energy. The proposed model is simulated using SOLIDWORKS and MATLAB/SIMULINK.

The rest of this paper is organized as follows. In Section 2, an overview of the proposed RPEH Systems is briefly explained. In Section 3, we present the prototype development and testing of the proposed RPEH system. The experimental results are also demonstrated and discussed. Section 4 concludes the paper. Finally, some topics for future work are shown in Section 5.

2. The Proposed RPEH System

Figure 1 illustrates the proposed road piezoelectric energy harvester (RPEH) system presented in our previous work [1]. When the vehicle stresses the piezoelectric module, placed underneath the road asphalt, an electrical AC signal is generated at the top-bottom sides of the piezoelectric module. The AC signal is then passed to the rectifier, and the harvested energy is stored temporally in a storage device. A data acquisition system (DAQ) and a computer are needed to capture the signals and study the harvester behaviors. Alternatively, an oscilloscope can be used to measure the output of the RPEH. However, there are concerns about the design. The main obstacle that was encountered was lab testing capacity. Therefore, the RPEH was shrunk to fit the testing equipment. The original harvester design featured an outer dimension of 9 inches. This was then shrunk to 4 inches. Additionally, the PZT stacks themselves had to be shrunk to accommodate the decreased diameter. Cost factors were also a limitation to the

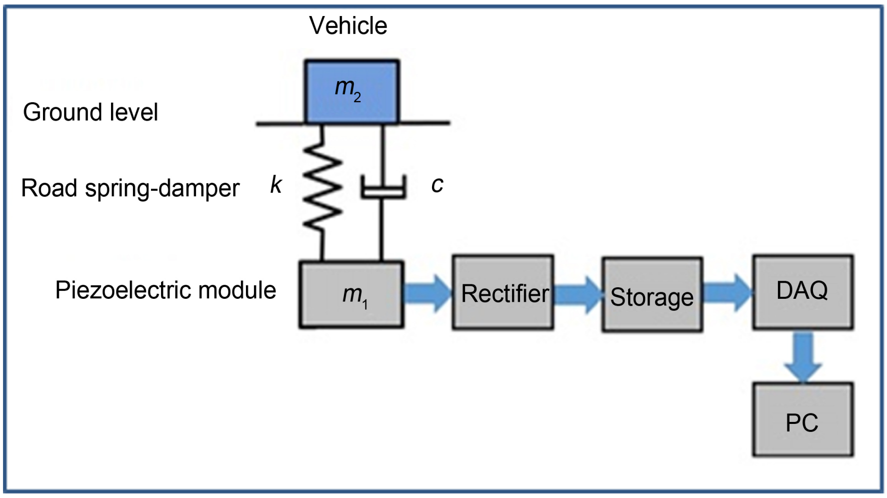

Figure 1. The proposed RPEH system [1].

design. Purchasing 5 or more pre-constructed stacks proportional to a harvester diameter of 9 inches would have exceeded the available budget for this project. Thus, our research purpose is to develop our previous design in [1] so that to harvest the optimized energy.

2.1. Mechanical Design and Solidworks 3D Model

There are three main components to a piezoelectric harvester: the piezoelectric themselves, a housing unit for the stacks, and an energy harvesting circuit. The PZT stacks used in this harvester consist of three layers of PZT-5H material with a diameter of 10 mm and thickness of 4.75 mm per layer, totaling a stack thickness of 14.25 mm. Five of these stacks are then housed in a polycarbonate unit with a 1018 AISI low carbon steel base plate. The stacks themselves are held in place using a small 3D printed stack holder made of PLA plastic. The purpose of this module is to maximize the stress distribution of the vehicle through the asphalt to the piezoelectric. The stacks are then wired in parallel and connected to an energy harvesting power electronic.

Table 1 illustrates the materials used for each component of the harvester. Figure 2 shows expanded view of harvester module with part name and material identified.

Polycarbonate Plastic:

The Top and Base Plates are both made from polycarbonate plastic. This material has several desirable material properties for this design. Some of these advantages are high resistance to impact force, high electrical insulator capability, easy machinability, and high stiffness.

Table 1. Material selection and advantages.

Material	Part(s) Constructed	Advantages
Polycarbonate Plastic	Top Plate Base Plate	Impact Resistance, Electrical Insulator, Machinability, High Stiffness
PLA Plastic	Stack Holder	3D Printing Capability Electrical Insulator
1018 AISI Low Carbon Steel	Support Plate	Machinability, High Stiffness, Inexpensive
PZT-5H	Piezo Stacks	Low Stiffness, High Piezoelectric-Performance
Neoprene Rubber	Spacer	Low Stiffness, High Elasticity High Fatigue Life Water Resistant

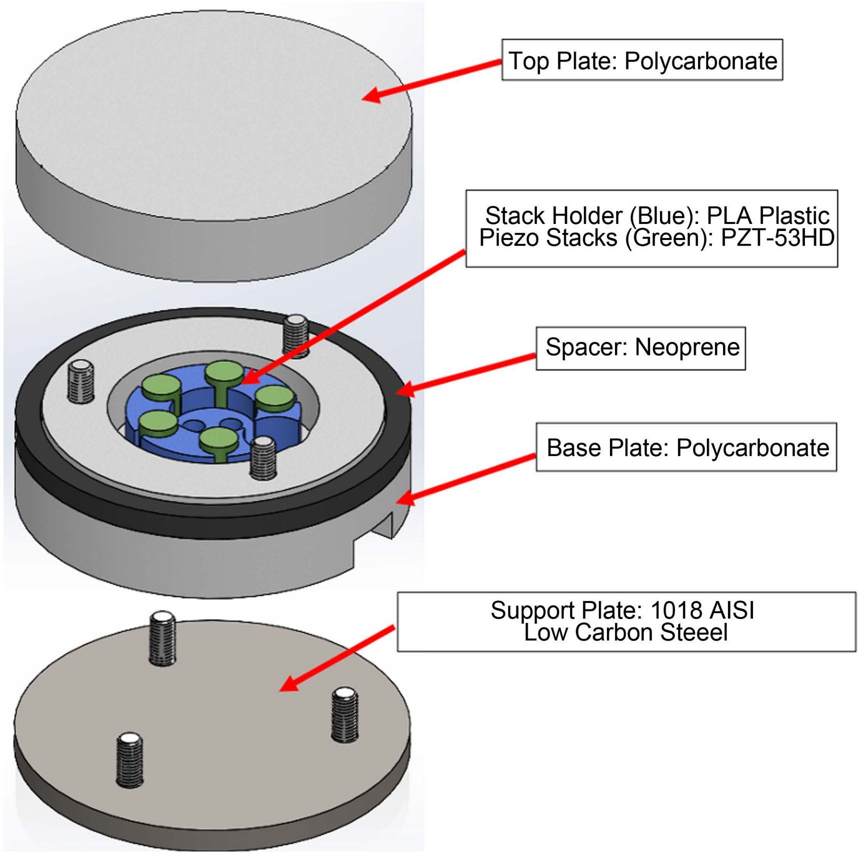

Figure 2. Expanded view of harvester module with part name and material identified.

It is critical for these parts to be rigid. Any deflection in these parts will result in a loss of harvested energy. Therefore, a material with high stiffness is needed. Vehicles will be passing over the Top Plate at potentially high speed. This can create a high impact on our module, so the material must be impact resistant to prevent damage. To prevent possible electrical shorts from the piezos, an electrically insulating material is desired. Not only is polycarbonate a good insulator, but it is less expensive and lighter than the same-sized steel. Since both the Top and Base Plate need to be CNC machined, machinability is a quality crucial for success which Polycarbonate is. Table 2 details the numerical values of polycarbonate material properties.

PLA Plastic:

The Stack Holder is made of Polylactic Acid (PLA) Plastic. This material was selected because of its use in 3D printing manufacturing. The Stack Holder does not have any applied forces to it, so its structural integrity is not critical. The piezo stacks will be housed in the Stack Holder, so to prevent potentially electrical shorts, a material that is an electric insulator is desired.

1018 AISI Low Carbon Steel:

The Support Plate is made from AISI 1018 low-carbon steel. This type of steel offers a good balance of toughness, strength, and ductility. The main function of the Support Plate is to add rigid support to the Base Plate and enclose the

Table 2. Polycarbonate material properties [2].

Mechanical Properties	Value	Units
Tensile Strength	6.55	MPa
Tensile Modulus of Elasticity	2.38	GPa
Tensile Elongation	%	135
Flexural Strength	93	MPa
Flexural Modulus of Elasticity	2.38	GPa
Compressive Strength	86.2	MPA

wires/fasteners. The Support Plate is also CNC machined, so machinability is crucial.

PZT-53HD:

The Piezo Stacks are the most essential component of the harvester. The stacks are made of zirconate titanate piezoelectric (PZT) ceramics. The specific material used for these stacks is PZT-53HD, manufactured by He-Shuai in China. PZT ceramics are preferred for their physical strength, chemical passivity, as well as their high operating temperature. These are highly desirable properties when considering the working conditions of the harvester. The properties of this material are specified in **Table 3**.

Neoprene Rubber:

The Spacer is made of neoprene rubber. Neoprene was selected due to its high elasticity, low stiffness, high fatigue life, and water resistance. High elasticity and low stiffness are desired to allow the Top Plate to "float" and return to its original position without permanently absorbing energy. The neoprene Spacer functions like a return spring. High fatigue life is important, so the Spacer does not wear out over time when loaded. Another function of the Spacer is to act as a gasket to prevent water from entering; therefore, high-water resistivity is desired.

Manufacturability:

The materials used to construct the harvester were chosen not only for their desired properties but their easy manufacturability. The 1018 AISI steel used in the support plate of the harvester provides a good balance of toughness, strength, and ductility. Additionally, steel was easily manufactured to the design specifications using a CNC (Computer Numerical Control) machine. This is the same reason why polycarbonate plastic was used for the toplayer and base plate. Polycarbonate is a strong, tough, and lightweight material and is easy to work with. A CNC machine was used to machine this plastic as well, shaping the material to the design specifications.

For the stack holder, PLA plastic and a 3D printer were used to manufacture the part. PLA plastic allows for a quick, cheap, and easy way to manufacture a part. This allows for easy redesigns if the part does not properly fit the PZT stacks, which have variations from the manufacturing process.

Table 3. PZT-53HD (5H, Navy VI) material properties [3].

Material Property	Symbol	Units	Value
Diameter	D	mm	10
Thickness	h	mm	5
Density	p	kg/m^3	7900
Yield Strength	Y	N/m^2	150×10^6
Piezoelectric Coefficient/Modulus	d_{33}	C/N	680×10^{-12}
Relative Permeability	s_{33}	/	3850
Electro-Mechanical Coupling Factor	k_{33}	/	0.74
Youngs Modulus	Y_{33}	N/m^2	8.9×10^{10}
Piezoelectric Capacitance	Cp	F	5.3×10^{-10}

Harvester Shape:

When conducting the literature review, it was apparent that most RPEHs are circular in design. This includes the harvester designs presented in [4] [5] [6]. The latter paper [6] tests both a square and circular harvester design. This paper concludes that a square design will produce more energy. However, this design was tested with the top of the harvester exposed and flushed with the road surface. When the harvester is installed under the asphalt, as is in this design manufactured for this project, the stress distribution from the tire through the road will be in a cone shape, this is discussed in a later section. Therefore, to maximize the harvested energy the harvester shape should be circular to match the conical stress distribution.

Burger's Model Asphalt Simulation:

Simulating asphalt in SIMULINK proved to be a difficult challenge. Developing a realistic mathematical model of asphalt is a complicated problem due to the complicated nature of asphalt mixtures which are susceptible to time-dependency, temperature, plastic flow in the binder, friction among particles, and the coupling of all these effects [7]. To formulate a constitutive description of viscoelastic materials one can also use differential formulation based on mechanical models. Mechanical models consisting of springs and dampers provide some physical insight into the viscoelastic behavior of materials. A widely used model of viscoelastic behavior for asphaltic materials is the Burgers model, shown in **Figure 3** [7]. The parameters of the Burger's model are shown in **Table 4**, when simulating the model, the average values were used and multiplied by the thickness of the asphalt to obtain the N/m and N/(m/s) units needed to input in the SIMULINK spring and damper blocks.

Determining Optimal Harvester Dimensions:

It is essential to optimize the diameter of the RPEH module, so the maximum amount of stress is applied. The optimal harvester diameter is directly related to the thickness of asphalt. The process below was used to determine the optimal

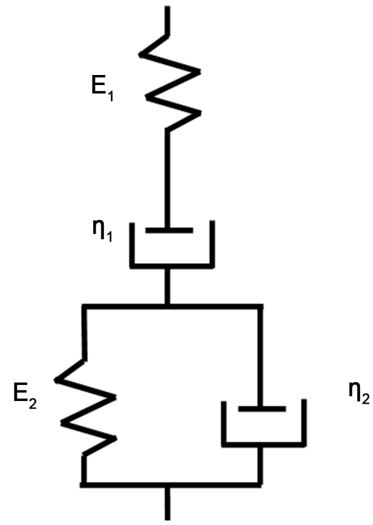

Figure 3. Burger's asphalt model [7].

Table 4. Parameters of the Burger's model [7].

20˚C	E_1, Mpa	E_2, Mpa	η_1, Mpa·s	η_2, Mpa·s
20 kN	247.77	6178.92	785.76	186.31
35 kN	461.25	2861.27	752.50	106.14
60 kN	229.30	2302.24	360.60	128.56
75 kN	286.91	2766.66	445.04	121.38
Avg.	306.31	3527.27	585.98	135.60

diameter. **Figure 4** shows a diagram of the stress distribution cone through a specified thickness of asphalt [8].

In this work, the values of t_A and D_T were selected as follows:

$$t_A = 5 \text{ cm} \tag{1}$$

$$D_T = 12.7 \text{ cm} \tag{2}$$

From **Figure 4**, (1), and (2), the stress distribution diameter, defined by D_B, can be computed as follows:

$$D_B = 2t_A + D_T = 22.7 \text{ cm} \tag{3}$$

Theoretical Stress on Stacks:

Once the optimal diameter was determined, the theoretical stress applied to the stacks can be determined using the process below. These calculations are important to make sure the piezos are not overstressed. The yield strength of the PZT-5H material is 150 MPa which is greater than the calculated theoretical stack stress of 1.45 MPa with a 1500 kg car input. The same calculations were made with a 36,000 kg car input, approximately the weight of a fully-loaded semitruck, this resulted in a 14 MPa theoretical stress, still underneath the 150 Mpa yield strength of the PZT-5H material.

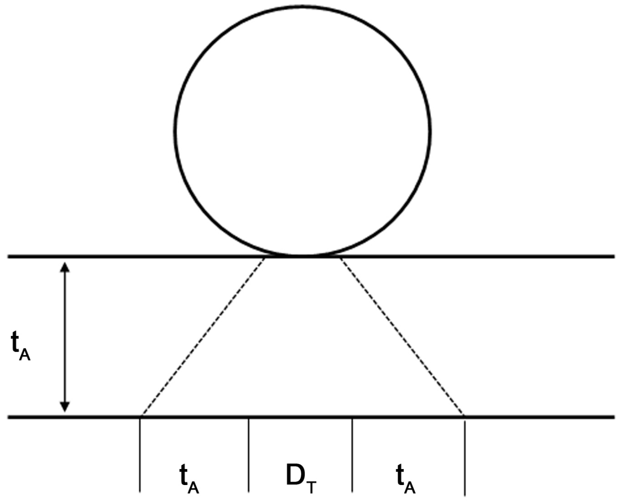

Figure 4. Stress distribution diagram. t_A is the Asphalt thickness. D_T is the tire footprint diameter thickness.

Optimal Module Diameter = 22.7 cm (from (3))

Defining the following parameters:

Testing Capacity Diameter = 10.16 cm

A_{tire} = Tire footprint area = 0.0161 m^2

W = average vehicle weight per tire

σ_T = Stress on top of asphalt

σ_B = Stress below asphalt

N_{Stack} = Number of stacks in module

F_{Module} = Resultant Force on top of Module

F_{Stack} = Resultant Force per Stack

σ_{Stack} = Stress Applied to Surface of Stacks

D_{Stack} = Diameter of Piezo Stack

A_{Stack} = Area of Stack

A_{Module} = Area of Module = 10.17 cm

Testing Module = 10.16 cm diameter:

Car Input (mass): 1500 kg

$$\sigma_T = \frac{W}{A_{tire}} = \frac{3679\ \text{N}}{0.0161} = 228.5\ \text{kPa} \tag{4}$$

$$\sigma_B = \sigma_T \frac{D_T^2}{D_B^2} = 228500 \frac{0.127^2}{0.2286^2} = 70.5\ \text{kPa} \tag{5}$$

$$F_{Module} = \sigma_B A_{Module} = 70500 \times \frac{\pi}{4} \times 0.1016^2 = 572\ \text{N} \tag{6}$$

$$F_{Stack} = \frac{F_{Module}}{N_{Stack}} = \frac{572}{5} = 114\ \text{N} \tag{7}$$

$$\sigma_{Stack} = \frac{F_{Stack}}{A_{Stack}} = \frac{114}{\frac{\pi}{4} \times 0.010^2} = 1.45\ \text{MPa} \tag{8}$$

Semi-Truck Input: 36,000 kg

$$\sigma_T = \frac{W}{A_{tire}} = \frac{35000\ \text{N}}{0.023} = 1.5\ \text{MPa} \tag{9}$$

$$\sigma_B = \sigma_T \frac{D_T^2}{D_B^2} = 1500000 \frac{0.153^2}{0.2286^2} = 0.7\ \text{Mpa} \tag{10}$$

$$F_{Module} = \sigma_B A_{Module} = 700000 \times \frac{\pi}{4} \times 0.1016^2 = 5.7\ \text{kN} \tag{11}$$

$$F_{Stack} = \frac{F_{Module}}{N_{Stack}} = \frac{5700}{5} = 1.1\ \text{kN} \tag{12}$$

$$\sigma_{Stack} = \frac{F_{Stack}}{A_{Stack}} = \frac{1100}{\frac{\pi}{4} \times 0.010^2} = 14\ \text{MPa} \tag{13}$$

2.2. Energy Conversion Principles of Piezoelectric

The main factors that affect the power output of a piezoelectric transducer are the piezoelectric material properties, the applied force, loading frequency, and the resistance of the connected load.

It can be proven from [4] that the output voltage V_P and the energy W produced by the piezo stack are given by

$$V_p = \frac{\alpha F h d_{33}}{n A_p \varepsilon_r} \tag{14}$$

$$W = \frac{d_{33}^2 \alpha^2 F^2 h}{2 n A_p \varepsilon_r} \tag{15}$$

where d_{33} is the piezoelectric strain constant, α is the force attenuation coefficient of the road, F is the vertical load stress, h is the thickness of piezoelectric ceramics.

It is clear from (1) and (2) that V_P and W are altered by both mechanical and electrical properties of the piezoelectric material. Optimization is required to address the device parameters that produce the maximum energy and voltage.

2.3. Optimization Using MATLAB/SIMULINK Simulation

SIMULINK and MATLAB were the primary programs used to simulate the RPEH. MATLAB was used to write a simple code that would allow the user to enter the harvester variables in the SIMULINK diagram. These input variables were then used in a SIMULINK block diagram, shown in **Figure 5(a)**. SIMULINK also has a premade piezoelectric stack block in its library. This block allows the user to easily change the number of layers, layer thickness, and diameter of the PZT stack. The layers in the PZT stack are connected in parallel. The stacks themselves are also connected in parallel. SIMULINK allows the user to generate a mechanical pulse, which is then converted into voltage through the PZT stack block. The mechanical pulse simulates the car tires driving over the

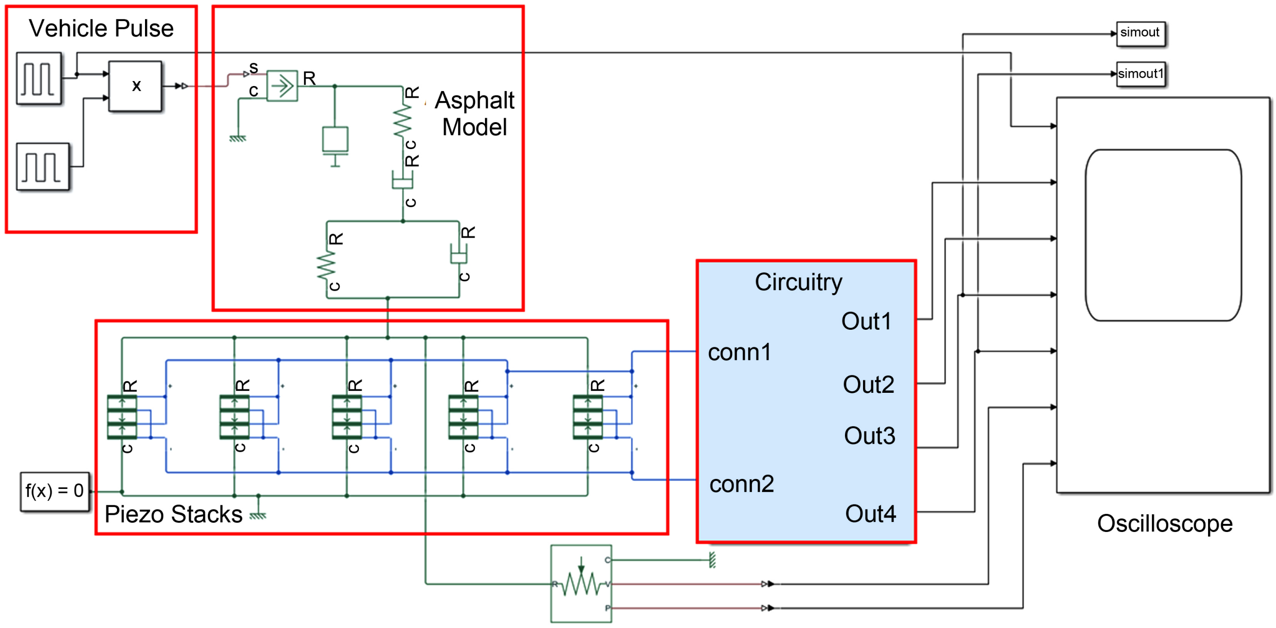

(a)

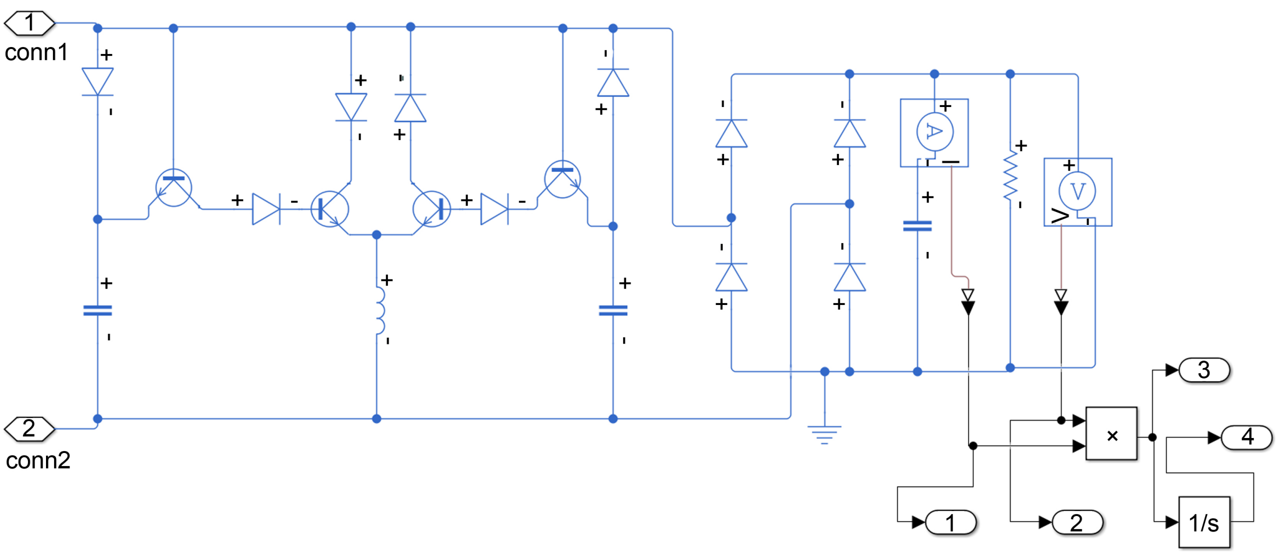

(b)

Figure 5. SIMULINK RPEH block diagram. (a): Block diagram; (b) SIMULINK SSHI rectifier circuit (circuitry block in (a)).

harvester. The RPEH Block diagram uses the burgers asphalt model, shown in Figure 3, to simulate the asphalt layer above the RPEH. Inside the circuitry subsystem (Figure 5(b)) is a Synchronized Switch Harvesting on Inductor (SSHI) rectifying circuit. This circuit serves as a high-efficiency rectifier, which converts the AC voltage produced by the PZT stacks into a DC voltage. The SSHI technique is based on the resonant circuit that is created by the internal capacitor of the piezoelectric stack and an external inductor which flips the capacitor voltage instantly to nullify the effect of the capacitive term. In this way, the energy used to charge the internal capacitor to conduct the diode bridge, which would have been wasted, is now harvested [9].

In this simulation, the DC voltage is then sent to a storage capacitor (470 μF), where the energy harvested per car was measured using the SIMULINK oscilloscope. It was based on this parameter that the optimum size of the PZT stacks was determined.

When determining the optimum thickness and number of layers per stack, a standard 15 mm total thickness was used, as well as a static 10 mm diameter. **Table 5** shows the results of the optimization after simulation. The highlighted values indicate the PZT stack size and layers that were used in this design.

Based off the SIMULINK results, the optimal stack dimensions are a diameter of 10 mm with 3 stack layers, each layer 4.75 mm thick. The resulting waveforms are shown in **Figure 6**. The voltage waveform was obtained by taking the voltage

Table 5. Results of the optimization after simulation.

No. of Layers	Thickness (mm)	Total Thickness (mm)	Diameter (mm)	V_{cap} (V)	E_{cap} (mJ)
15	1	15	10	19.90	0.0938
5	3	15	10	19.80	0.0920
3	5	15	10	20.10	0.0949
2	7.5	15	10	19.83	0.0924
1	15	15	10	19.94	0.0936

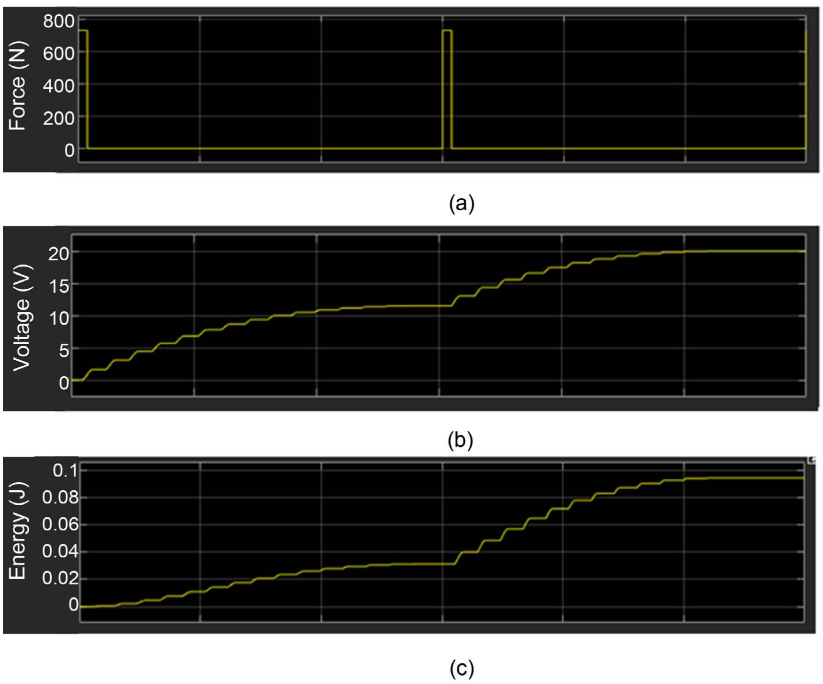

Figure 6. SIMULINK Results 3 layers, 5 mm thickness using one care passing that stresses the piezoelectric module using the front and the back tires. (a) Force per Stack (N); (b) Storage Capacitor Voltage (V); (c) Storage Capacitor Energy (J).

across the load resistor and thus the parallel load capacitor. The harvested electrical energy W stored in the capacitance C was then calculated as follows:

$$W = \frac{1}{2} \times C \times V_c^2 \tag{16}$$

where V_c is the voltage across the capacitor.

3. Prototype Development and Testing

Figure 7 shows the completed RPEH with a fully assembled view and an inside view with the PZT stacks wired in parallel. Figure 8 alternatively shows a deconstructed view of the harvester with labeled parts.

(a) (b)

Figure 7. Completed RPEH prototype. (a) The five stacks installed in RPEH; (b) Assembled RPEH.

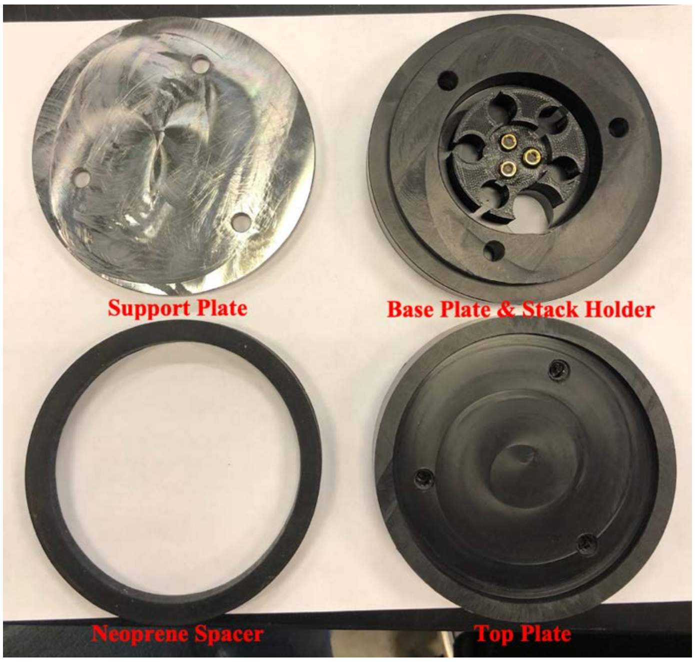

Figure 8. Disassembled RPEH with labeled parts.

The manufacture of the harvester went smoothly, with only minimal modifications needed. The Top Plate, Base Plate, and Support Plate were all manufactured using the CNC machine. This allowed for the harvester parts to be manufactured to the exact design specifications.

The neoprene spacer was manufactured by shearing the teeth off two-hole saws, creating a sharp edge, with outer diameters of 10.48 cm and 9.53 cm respectively. A sheet of neoprene was then placed underneath the hole saw in a hydraulic press to cut out a circle of neoprene. This process was repeated for the smaller hole saw with the neoprene circle to create the neoprene ring.

The PZT stack holder was manufactured by using a 3D printer. Small metal threads were embedded into the PLA plastic stack holder by use of a soldering iron. These threads allowed for the stack holder to be bolted to the base plate.

Once the stack holder was fastened to the base plate the PZT stacks were fit into the slots, and the wire leads of the stacks were soldered in parallel. The stack wires were then soldered to a larger wire with two leads. The exposed stack wires were then wrapped in a heat shrinking plastic.

Modifications:

The stack holder had to be 3D printed multiple times while adjusting the piezo hole diameters. This hole diameter is crucial to allow for proper fitment of the PZT stacks. If the hole diameter is too large, the stacks will be able to rotate, which is undesirable. If the holes if too small, then the stacks won't fit. It is also difficult to get all piezo stacks to fit identical with part diameter variation from the supplier.

After installing the PZT stacks, the clearance must be set between the top of the stacks and the contact area of the Top Plate. This is important because the PZT stacks must be in contact with the Top Plate when the bolts are tightened while simultaneously allowing enough crush in the neoprene spacer to provide a sufficient seal. An additional 0.040 of material had to be removed from the Top Plate to allow more crushing of the Neoprene Spacer. The Top Plate modification can be viewed in **Figure 9**.

Figure 9. Top plate with added clearance.

The piezo stack connection where all stacks were soldered together was initially done outside the module. This was done to easily check connection joints if troubleshooting was needed. This, however, was a bad idea because solder connections broke when tamping the asphalt down during installation due to the stiffness of the solder. To correct this error, the connections were resoldered and relocated inside the module. This offered protection to the joints, so no stress was applied.

3.1. Wheel Tracking Asphalt Testing

The RPEH was tested using a Hamburg Wheel Tracking machine. This machine is used in AASHTO-T324 asphalt testing to simulate road loading conditions and to test the permanent deformation resistance of the asphalt layer. The wheel tracking machine applied a force of approximately 700N to the asphalt at a speed of 1.6 km/h. The 700N force would be divided amongst the five stacks to total an approximate force of 140N per stack.

The RPEH was embedded in "Aquaphalt" which is a cold compacting asphalt mix used in driveway repairs. Cold compacting asphalt was used in this test as the harvester cannot be embedded in a hot mix of asphalt. The embedding process is shown in **Figure 10**.

After the RPEH was embedded in the Aquaphalt, it was left to cure for 24+ hours to allow the mix to stiffen. Once the RPEH was installed into the mold and underneath "Aquaphalt" it was then put into the Hamburg Wheel Tracking machine. The wheel tracking machine, with the embedded RPEH, is shown in **Figure 11**. The RPEH then was tested with an open circuit and with a load R_L equals to 10 kΩ, 100 kΩ, 500 kΩ, 600 kΩ, 900 kΩ, 1 MΩ and 10 MΩ. The peak voltage V_L across R_L is recorded. Then, the peak instantaneous power $P_{L(peak)}$ delivered to the load is given by:

$$P_{L(peak)} = \frac{V_L^2}{R_L} \tag{17}$$

3.2. Results

After running the tests using the wheel tracking machine, **Figure 12** shows the results. This includes the instantaneous peak voltage for each tested resistor, as well as the peak instantaneous power. These are visualized by the blue bar graph, and the orange line plot, respectively. Additionally, an estimated power curve was included on the graph in orange. During testing, connecting a 900 kΩ resistor to the RPEH yielded the highest power output; however, a value of 950 kΩ would most likely yield a slightly higher value, as predicted by the curve.

Additionally, the oscilloscope data obtained during the asphalt test was imported into MATLAB to calculate the transient energy harvested per one loading pass. This was accomplished by using the "xlsread" function to import the oscilloscope ".csv" files into MATLAB. Following that the "trapz" function was used to calculate the area under the power curve, energy. These values were then

Figure 10. (a) Layering Aquaphalt on top of RPEH; (b) Compacting Aquaphalt; (c) Tamping surface Aquaphalt layer; (d) RPEH embedded under Aquaphalt.

plotted in Figure 13. The process was done to obtain results that could be compared more easily to the SIMULINK simulation results. The plot implies that at a resistor load of 600 kΩ a max energy of 45 uJ was harvested.

3.3. Discussion: Simulations Vs Experimental

The SIMULINK simulation, used to optimize the PZT stacks, best represents the RPEH in actual road conditions because of the force applied to the harvester, as well as the Burger's asphalt model. These results show an approximate 20 V collected in the storage capacitor, equating in 0.0949 J of energy. This simulation was run using the SSHI rectifier circuit as explained in Section 2.2.

The wheel tracking asphalt test was conducted to observe if the RPEH would function underneath asphalt, which it succeeded in. When testing the RPEH

(a) (b)

Figure 11. (a) RPEH in Hamburg wheel tracker; (b) Hamburg wheel tracker running.

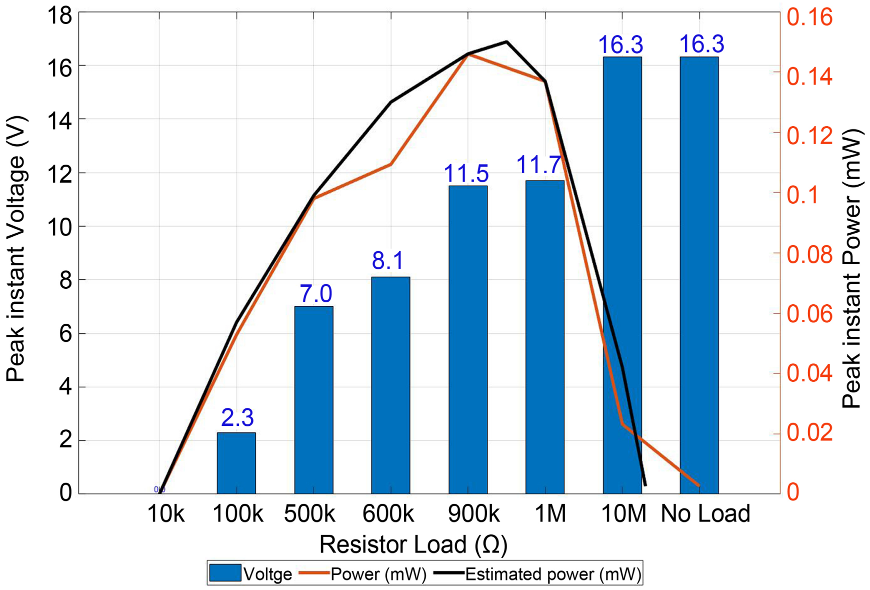

Figure 12. Instantaneous peak voltage and power for varying resistor loads (asphalt test).

with the wheel tracking machine, varying resistor loads where connected to the output of the RPEH, this was done to observe the power curve, and determine the optimum resistor load. This was determined to be 950 kΩ. Additionally, MATLAB was used to calculate the energy harvested by the RPEH with each resistor attached. A max energy for this test was obtained from the 600 kΩ resistor connected to the RPEH, totaling in 45 μJ harvested. This value is much lower than the simulated energy output of 94.9 mJ, however, there are varying factors

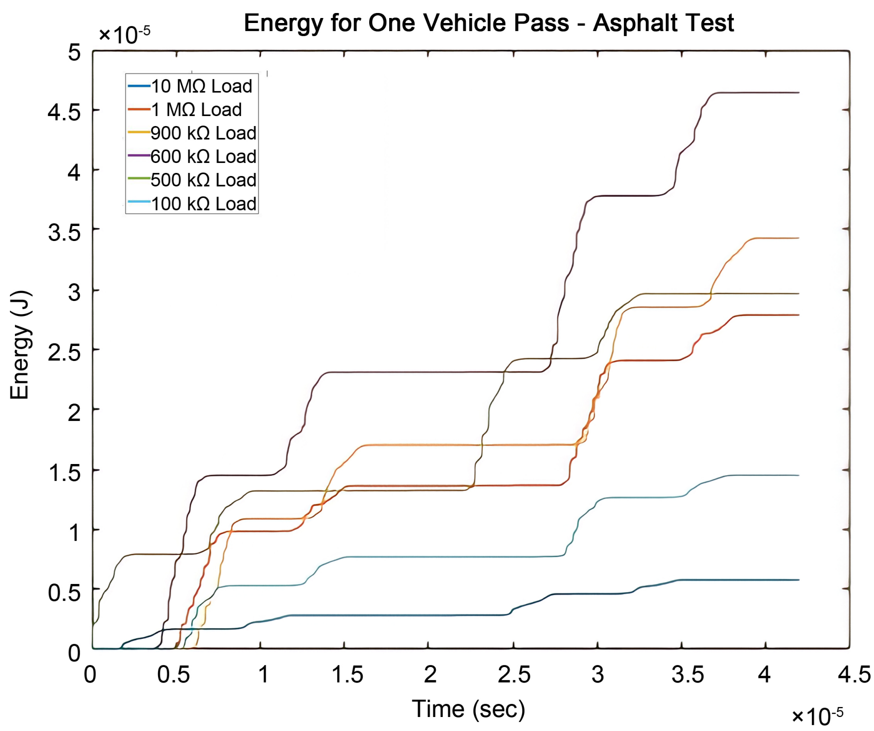

Figure 13. Transient energy for one vehicle pass-asphalt test.

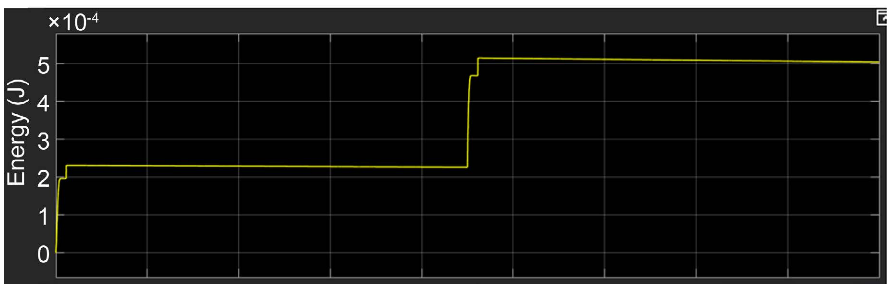

Figure 14. SIMULINK simulation energy results to compare to asphalt test.

that could have affected this change. Chiefly, the force used in the simulation was much higher than that of the asphalt test, approximately 700N compared to approximately 140N, respectively. This force was also applied at a greater speed in the simulations, about 120 km/h compared to the 1.6 km/h of the wheel tracking machine.

Therefore, a second SIMULINK simulation was run with input variables to match that of the wheel tracking machine. This included a load of 140N per stack at a speed of 1.6 km/h. Figure 14 shows the stored energy inside the load capacitor after a single pass.

The results of this simulation show an output of 500 μJ per car pass, this value is still larger than the 45 μJ calculated energy output during asphalt testing. However, there are a few factors that could differentiate the two outputs. First, the simulation was once again conducted using an efficient SSHI rectifying circuit, while the actual asphalt testing only applied varying resistor loads to the

RPEH. Secondly, the simulation does not factor in the material properties of the neoprene spacer, this is most likely the cause of differing outputs as some energy had to be lost through this part. And lastly, the simulation uses the Burger's asphalt model to simulate asphalt, during testing "Aquaphalt" was used in place of traditional asphalt found in a road. It is unclear which of these factors contributed the most to this lowered output, but it is apparent that these are the reasons.

4. Conclusions

This project achieved its goal of proving the theory that piezoelectric energy harvesting is achievable. The prototype RPEH successfully harvested mechanically induced stresses through the asphalt from simulated road traffic and converted this energy into usable low-power electrical energy. This project, however, needs more research to carry out the feasibility in real-world applications.

The mechanical design was thoroughly completed; however, a custom power electronic for the RPEH was unable to be completed. Due to the time limitations, a custom circuit couldn't be designed, so an off-the shelf-energy harvester board was purchased. This board worked great to show the charge pumping theory and usability of the harvested energy.

To conclude, this project was successful in developing and testing a prototype Road-Compatible Piezoelectric Energy Harvesting device, despite missteps. A research paper was written on the work conducted during the fall semester and recently published [1]. The prototype RPEH was presented and demonstrated at the Penn State Altoona Undergraduate Research Fair, placing 2nd in engineering, as well as 3rd for the sustainability award. This project shows that piezoelectric energy harvesting is a good low power, green energy source; and sets the stage for future work to be conducted for this project.

5. Future work

For future work, it is recommended to test a full-size harvester underneath real asphalt to simulate the true working conditions of the RPEH. To accomplish this, the prototype harvester presented in this report should be up scaled to a diameter of 9 inches to make full use of the stress distribution cone while under 2 inches of asphalt. This will also require the PZT stack sizes to be reoptimized to match the increased harvester diameter.

Also, a suggestion for future works is to create another module made from a high temp resistant and high stiffness epoxy instead of using polycarbonate plastic. This will provide better energy transfer because of the increased hardness and allow us to use hot mix asphalt during testing.

Along with the increased RPEH size, it is also recommended that a custom power electronic with a rectifier and DC/DC converter be developed to increase the harvesting capabilities of the RPEH. This would aid in the RPEH's efficiency in harvesting electrical energy, as well as powering a low-power electronic.

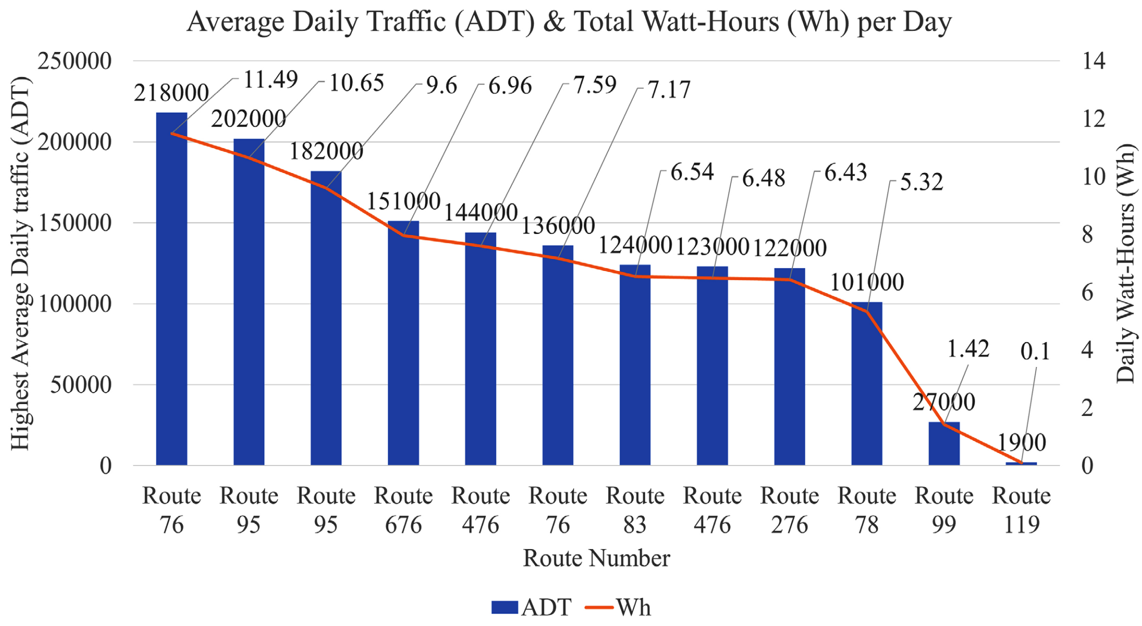

Figure 15. Average Daily Traffic (ADT) & Total Watt-Hours (Wh) per day per route.

A major issue for future work would be the actual implementation of the device, as obtaining permission to install the harvester under the asphalt could prove difficult. Proper permission to test the RPEH in a roadway would have to be obtained well before testing begins.

To simulate the actual road implementation of the RPEH designed in this report, an analysis of the average daily traffic values for some of the busiest routes in Pennsylvania was conducted. This data was collected during 2020 and is provided by the Pennsylvania Department of Transportation [10]. **Figure 15** shows the highest average daily traffic (ADT) values for routes in Pennsylvania, and the corresponding power harvested per day, in watt-hours. Additionally, I99 has been included to act as a reference point, and Route 119 has the lowest traffic volume and power harvested per day. The results of these graphs clearly state that a road with a higher traffic volume will produce a greater power yield per day.

To calculate the total daily watt hours harvested, the results from the SIMULINK simulation were used, as they best simulate the force of a car applied to the RPEH. The total energy collected for one RPEH after one car pass (two-wheel passes) was 0.0949 J. This value was multiplied by 2 as there would be an RPEH for each side of the car. The following Equation (18) was then used to calculate the total energy in watt-hours collected per day.

$$\text{Total Daily Watthours} = \frac{(\text{Total Energy per Car})(\text{ADT})}{3600 \text{ seconds}} \tag{18}$$

Acknowledgements

This work is funded by Pennsylvania State University, under the undergraduate research grant (URG) and the research development grant (RDG).

Conflicts of Interest

The authors declare no conflicts of interest regarding the publication of this paper.

References

[1] Sherren, A., Fink, K., Eshelman, J., Taha, L., Anwar, S. and Brennecke, C. (2022) Design and Modelling of Piezoelectric Road Energy Harvesting. *Open Journal of Energy Efficiency*, **11**, 24-36. https://doi.org/10.4236/ojee.2022.112003

[2] Polycarbonate Properties. Curbell Plastics. https://www.curbellplastics.com/Research-Solutions/Plastic-Material-Properties/Polycarbonate

[3] He-Shuai LTD (2018) Hard PZT & Soft PZT Data Sheet. Aug. 1st, 2018.

[4] Zhang, W.J., Ding, G.Y. and Wang, J. (2021) Road Energy Harvesting Characteristics of Damage-Resistant Stacked Piezoelectric Ceramics. *Ferroelectrics*, **570**, 37-56. https://doi.org/10.1080/00150193.2020.1839254

[5] Wang, J., Liu, Z.M., Ding, G.Y., *et al.* (2021) Watt-Level Road-Compatible Piezoelectric Energy Harvester for LED-Induced Lamp System. *Energy*, **229**, Article ID: 120685. https://doi.org/10.1016/j.energy.2021.120685

[6] Yang, H., Wei, Y., Zhang, W., Ai, Y., Ye, Z. and Wang, L. (2021) Development of Piezoelectric Energy Harvester System through Optimizing Multiple Structural Parameters. *Sensors*, **21**, Article No. 2876. https://doi.org/10.3390/s21082876

[7] Lewandowski, R. and Pawlak, Z. (2012) Optimal Placement of Viscoelastic Dampers Represented by the Classical and Fractional Rheological Models. In: Lagaros, N., Plevris, V., *et al.*, Eds., *Design Optimization of Active and Passive Structural Control Systems*, IGI Global, Hershey, Pennsylvania, 50-84. https://doi.org/10.4018/978-1-4666-2029-2.ch003

[8] Leiva-Villacorta, F., Vargas-Nordcbeck, A., Aguiar-Moya, J. P. and Loría-Salazar, L. (2016) Influence of Tire Footprint Area and Pressure Distribution on Pavement Responses. In: Aguiar-Moya, J., Vargas-Nordcbeck, A., *et al.*, Eds., *The Roles of Accelerated Pavement Testing in Pavement Sustainability*, Springer, Cham, 685-700. https://doi.org/10.1007/978-3-319-42797-3_45

[9] Covaci, C. and Gontean, A. (2020) Piezoelectric Energy Harvesting Solutions: A Review. *Sensors*, **20**, Article No. 3512. https://doi.org/10.3390/s20123512

[10] https://www.penndot.pa.gov/ProjectAndPrograms/Planning/TrafficInformation/Pages/2020-Pennsylvania-Traffic-Data.aspx